

Citation for published version:

Scobie, J, Shelley, W, Jackson, R, Hughes, S & Lock, G 2020, 'Practical perspective of cricket ball swing', *Proceedings of the Institution of Mechanical Engineers, Part P: Journal of Sports Engineering and Technology*, vol. 234, no. 1, pp. 59-71. <https://doi.org/10.1177/1754337119872874>

DOI:

[10.1177/1754337119872874](https://doi.org/10.1177/1754337119872874)

Publication date:

2020

Document Version

Peer reviewed version

[Link to publication](#)

James Scobie et al, Practical perspective of cricket ball swing, *Proceedings of the Institution of Mechanical Engineers, Part P: Journal of Sports Engineering and Technology* (Journal Volume Number and Issue Number) pp. xx-xx. Copyright © 2019. Reprinted by permission of SAGE Publications.

University of Bath

Alternative formats

If you require this document in an alternative format, please contact:
openaccess@bath.ac.uk

General rights

Copyright and moral rights for the publications made accessible in the public portal are retained by the authors and/or other copyright owners and it is a condition of accessing publications that users recognise and abide by the legal requirements associated with these rights.

Take down policy

If you believe that this document breaches copyright please contact us providing details, and we will remove access to the work immediately and investigate your claim.

JA Scobie¹, WP Shelley¹, RW Jackson¹, SP Hughes² and GD Lock¹

¹Department of Mechanical Engineering, University of Bath

²The Analyst, Editor of the Cricketer Magazine

Practical Perspective of Cricket Ball Swing

Abstract

A cricket ball has an encircling, stitched seam proud from the leather, separating the surface into two distinct hemispheres. When angled, this seam is exploited by the skilful bowler to create an asymmetry in the viscous boundary layer and the ball will *swing*. In this paper, the fluid dynamics of both *Conventional Swing* (CS) and *Reverse Swing* (RS) are explained and demonstrated. Using balls worn under match conditions and insight from a professional cricketer, factors affecting swing were tested experimentally in a wind tunnel. The *surface condition* of the ball was demonstrated to have a substantial effect on the amount of swing: CS was most obvious for a new, polished cricket ball and the swing reduced as the ball accumulated wear as would happen as the match progresses; RS was seen at high bowling speeds with a worn ball. *Humidity* in isolation was shown to have no significant effect on swing, dispelling a long-standing myth in the cricketing community. A grid was used to simulate *atmospheric convective micro-turbulence* above a cricket pitch on a hot day without cloud cover; strong evidence suggested that turbulence inhibits the fragile conditions necessary for laminar flow and prevents swing.

1 Introduction

Cricket has developed rapidly from an isolated rural game in the 16th century to a global sport [1]. The premise of cricket is relatively simple and is not dissimilar to other bat and ball sports such as baseball: a hard, leather-covered ball is projected towards a batsman who must try to score *runs* by hitting it past ten opposition players in a large oval field. To someone with limited knowledge of the game, cricket can seem inert, repetitive, confusing and slow-paced. However, an understanding of the hidden nuances and tactics which influence and shape a match, which evolves over the course of days, reveals the excitement and strategy of the game.

It is well known that footballs, baseballs and tennis balls *swerve* in flight. This is the *Magnus effect*: although the balls are geometrically symmetric, spin imparted onto the ball creates an asymmetry in the flow and differences in pressure create an aerodynamic force that causes the ball to swerve [2]. In contrast, the *swing* of a cricket ball fundamentally depends on the asymmetry of the ball itself. The encircling seam separates the ball into two distinct hemispheres and differences in the behaviour of the associated viscous boundary layers. (Note that there are also two secondary seams which are internally stitched and situated at 90° to the primary seam - these can influence the fluid dynamics, but are of second-order effect).

Swing bowling requires skill and experience. A skilful bowler can generate effective swing if the ball is delivered at pace with the primary seam angled slightly to an upright position. The ball is bowled with the bowler's index and middle finger either side of this seam. By imparting a small backspin, the bowler can generate enough gyroscopic inertia to stabilise the seam position during the trajectory of the ball; a wobbling seam will mean no swing. In Test matches, effective swing is associated with a release-speed in excess of 80 mph (> 36 m/s) from the bowler's hand [3]. *Conventional swing* (CS) usually occurs with the new ball, at the start of the match, and can sometimes mysteriously disappear after a few overs. *Reverse swing* (RS) occurs as the ball wears and the surface deteriorates, typically occurring after 25-30 overs; here the ball will swing exactly the opposite way to the conventional form and can only be achieved by the faster bowlers. The rough and smooth sides of the ball for CS and RS are illustrated in Fig. 1. Faster bowlers can exploit the phenomenon of *late swing* to deceive the batsman, where the natural deceleration due to drag will create the aerodynamic conditions for effective swing only late in the trajectory.

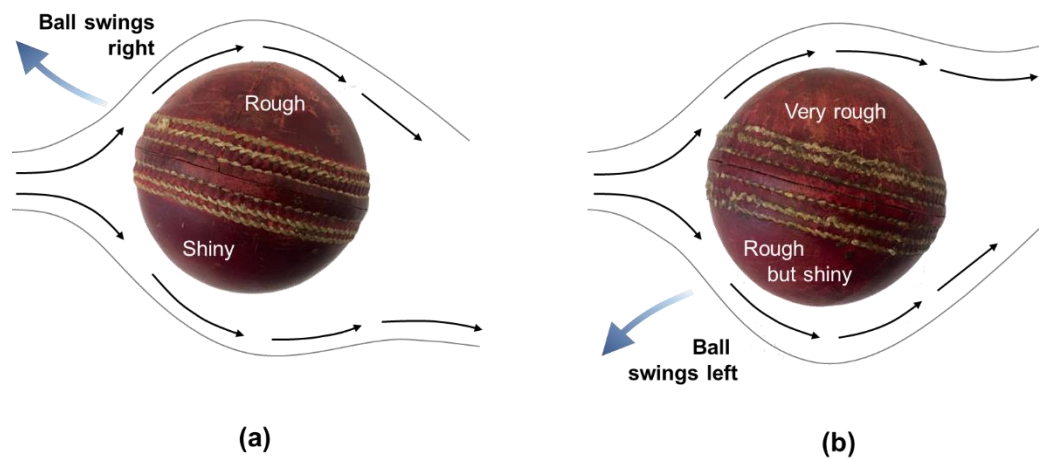


Figure 1: Conventional Swing (a) and Reverse Swing (b) as shown from above

The most skilful bowlers cannot guarantee swing, as it is not solely due to the bowler's technique and ability. In a recent interview, James Anderson (who holds the world record for Test wickets for a fast/swing bowler) discussed the mysterious nature of swing, emphasising that local weather and ground conditions were important. Cricketers will often refer to the weather as they make tactical decisions. There is a huge diversity in the atmospheric conditions and the texture of playing fields around the globe. Swing is elusive. It tends to happen on cloudy days, but not sunny days, and at particular grounds (*e.g.* Trent Bridge), but not others. Further, Test cricket uses red balls, recent day-night cricket has introduced pink balls, twilight and dew, while limited-over cricket uses white balls. There are different manufacturers (*Dukes, Kookaburra*) that produce balls with variations in the texture of the leather. Red balls are manufactured using aniline leather, where the material is dyed without using a polymer topcoat of insoluble pigments. In contrast, pink-ball leather is pigmented with a polymer topcoat [4]. *Dukes* balls are generally used in the UK with some increased use in Australia in recent years.

Even the most skilful bowlers probably do not fully understand the nuances and causes of swing, especially over the wide-range of conditions experienced during a five-day Test match. The condition of the surface of the ball is known to be crucial and during

the course of play the fielding side will vigorously polish one side of the ball. Reverse swing happens with a roughened, older, worn ball [5]. Cricketers will manipulate the ball to help generate swing, by means fair and foul. The laws of cricket forbid altering the surface condition with foreign objects. Recently, several high-profile cricketers have received bans for foul-play. In March 2018, Australian players attempted to gain an advantage using sandpaper to roughen the ball to summon reverse swing; and there have been many instances of polishing with saliva after sucking sweets to add an effective *lacquer* to the surface and prolong conventional swing.

The romantic cricket enthusiast loves the enigmatic and clandestine nature of swing, the *Black Art* of cricket. If the fielders can conjure it in the depth of an innings, then controversy, drama and a decisive advantage may follow. The rational cricket enthusiast would wish the mystery and subterfuge explained using cold logic, as in a good Sherlock Holmes story. Swing provides something for everyone.

The aim of this paper is to measure the side force, which quantifies the force causing swing, of cricket balls from different manufacturers (*Dukes, Kookaburra*) and of different colour (red, white, pink). The measurements are taken over a full range of bowling speeds encountered in first-class conditions. The paper also investigates the effects of aging (in terms of overs bowled), using balls worn under match conditions and insight from a professional cricketer. The effects of humidity and turbulence on swing are also measured. Appendix 1 provides a table identifying each factor affecting swing and linking it to the relevant graph in the Results section. The research question: how do these different factors link to the fundamental, governing fluid dynamics?

2 Literature review of the fluid dynamics of swing

The earliest academic paper documenting the lateral movement of cricket balls was published by Cooke [6] in 1955. Lyttleton [7] postulated a theory in 1957 (described below) which is now widely accepted as the first thorough explanation for conventional swing, though he attempted no experimentation himself. In his classic book *The Art of Cricket* [8], Don Bradman published a part of a talk given by Lyttleton on the BBC in which topics such as late swing and the effect of weather were discussed. A relatively recent review of cricket-ball swing was published by Mehta [9]

Conventional swing is well understood and illustrated in Fig. 2 [10] with the encircling primary seam inclined at an angle to the flow. The fluid-dynamic boundary layer separates from the surface of the ball as it experiences an adverse pressure gradient. On the seam side of the ball, the flow has been tripped into turbulence. On the non-seam side of the hemisphere, the flow is laminar. The turbulent boundary layer, by virtue of its increased momentum, remains attached up to a greater angle ($\approx 120^\circ$) compared to the undisturbed laminar side ($\approx 80^\circ$). The asymmetrical separation leads to a pressure distribution that creates a net aerodynamic force on the ball perpendicular to the flight trajectory.

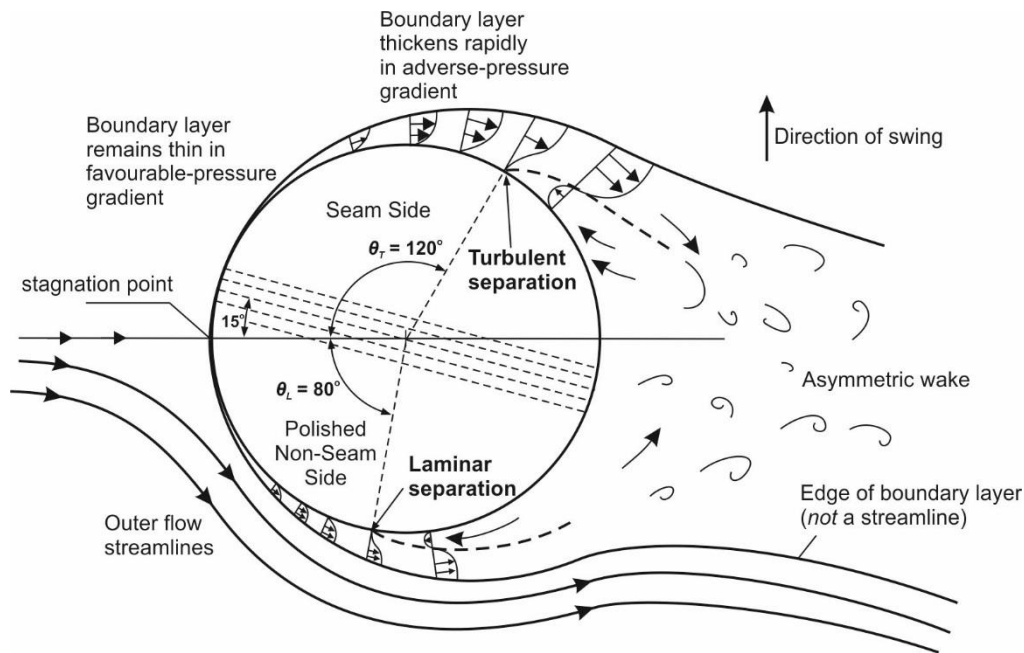


Figure 2: Conventional Swing (CS) of a cricket ball (boundary layer greatly exaggerated for clarity) as shown from above

For typical pace bowlers, conventional swing usually occurs with the new ball, early in the innings. At the start, the ball has a shiny, smooth, lacquered surface that encourages the laminar flow on the side opposite the seam. Laminar flow is fragile. The ball will wear and roughen as the match progresses, causing natural transition to turbulent flow - there is turbulent flow on both sides, so the asymmetry and swing are lost as the ball ages with play. During the course of play, the fielding side will vigorously polish the ball to maintain this smooth condition and prolong the period where swing is effective – the polished side opposite the seam is marked in Fig. 2. On a sunny day the sun will warm the wicket and generate micro-turbulence [11], which may disturb the laminar flow and transform it to turbulence – hence swing tends to happen on cloudy days, not sunny days [12]. It could be that the stands, shadows and cross breezes in some grounds may create the right local, micro-climate for quiescence and encourage laminar flow; this establishes some cricket grounds with a reputation for swing.

Cricket was introduced controversially to reverse swing in the late 1980s and early 1990s. At first esoteric, it was exploited by a new generation of bowlers from Pakistan who could consistently bowl at speeds in excess of 85 mph. With RS, the ball will swing exactly the opposite way to the conventional form and the phenomenon is associated not with the shiny, new ball, but one roughened during the course of play. It is no coincidence that cricket pitches in Pakistan are traditionally dry and abrasive. Reverse swing is now ubiquitous, but still courts mystery, drama and controversy.

Reverse swing is usually obtained when the non-seam side has aged and taken on a degree of roughness (Fig. 1). The side with the seam may also roughen, but it is the non-seam side that governs RS. From a fluid-dynamic perspective, Scobie *et al.* [10] were the first to postulate and experimentally observe that the reversed asymmetric pressure force driving RS is due to a laminar separation bubble (LSB) on the non-seam side of the ball. This has been recently verified by Deshpande *et al.* [13]. The LSB for

reverse swing is illustrated schematically in Fig. 3. There is turbulent separation on the seam side as before due to prominent primary seam. As discussed below, the roughened surface on the non-seam side will experience a boundary layer that separates, then reattaches downstream of the bubble, further downstream than the turbulent separation on the side with the seam.

It is possible to obtain RS with a new, pristine, ball at extreme pace. The data collected in this paper shows that a new, red *Dukes* ball will RS at 95+ mph.

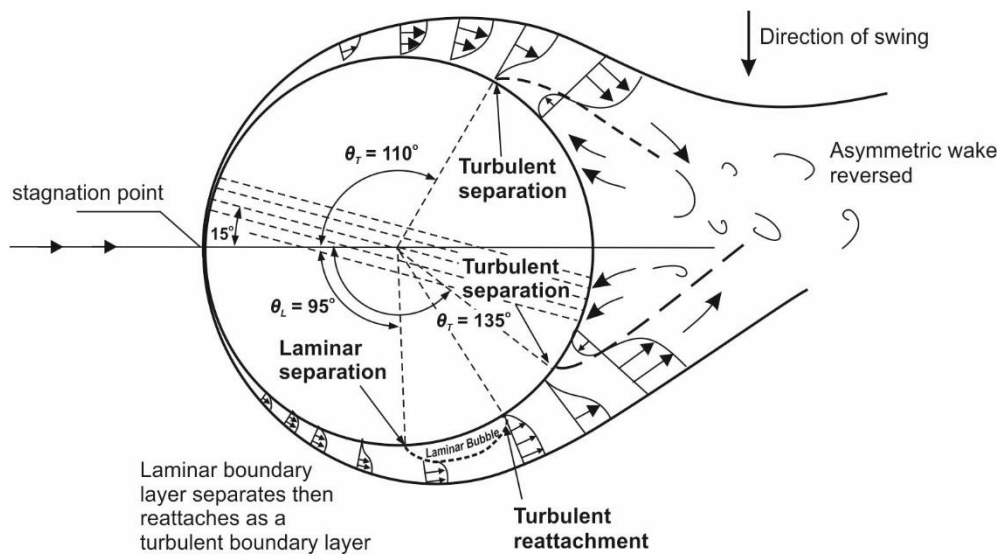


Figure 3: Reverse Swing (RS) of a cricket ball (boundary layer greatly exaggerated for clarity) as shown from above

2.1 Atmospheric conditions

Cricketers and commentators often discuss the effect of the atmospheric environment on swing. The general wisdom is that swing is more likely in cloudy, humid conditions and less likely on hot, sunny days. In the laboratory, Horlock [14] noted in his study of CS that levels of humidity had no effect on the magnitude of the measured swing-force. Sherwin and Sproston [15] varied the humidity values between 61% and 100% and also found no effect on the magnitude of swing. Daish [16] suggested that the stitching of the seam may swell under highly-humid conditions, but Bentley *et al.* [17] tested this theory and found no correlation between humidity and the seam swelling.

Sherwin and Sproston [15] suggested that atmospheric turbulence rather than humidity, may be an explanation for decreased swing on sunny days. Clearly, the formation of the laminar boundary layer on the smooth side of the ball is crucial for effective CS, and not possible in the presence of turbulence. Cloud cover will reduce the direct irradiation and heating of the wicket by the sun; this will reduce any micro-turbulence generated by warm air rising from the ground, allowing the fragile laminar boundary layer to form naturally. The dryness of the ground and the temperature are also important, as discussed by Wilkins [12] who presents typical levels of micro-turbulence in the atmosphere due to heating from the sun.

2.2 Cricket balls and roughness

A range of cricket balls were used in this study. Red and pink new balls were supplied directly by *Dukes* and white balls were supplied by *Kookaburra*. A series of red balls worn between 8 – 80 overs under first-class conditions were supplied by Warwickshire County Cricket Club. In addition, pink (*Kookaburra*) balls worn under first-class conditions were provided from an MCC day-night match. Photographs of the new red and pink *Dukes*, the new white *Kookaburra*, and the red balls aged after 8-10, 25, and 40-50 overs are shown in Fig. 4. More detailed photographs of all the balls are shown in Appendix 2. Note that the fielding side are offered a new ball after 80 overs. The diameter (d) of all of the balls, excluding the seam, were in the range $71.3 \text{ mm} < d < 71.9 \text{ mm}$. For the red and pink *Dukes* balls and the white *Kookaburra* balls, the seam dimension proud of the surface (k_s) was $\sim 1 \text{ mm}$. The size of the surface roughness (k_r) on the worn, scuffed balls was hugely variable, but estimated to an order of magnitude lower even for the balls aged to 80 overs. For the context of the discussion below, $k_s/d \sim 1000 \times 10^{-5}$ and $k_r/d \sim 100 \times 10^{-5}$.



Figure 4: Images of cricket balls tested

2.3 Boundary-layer separation around smooth spheres

The definitive study of the fluid-dynamic boundary layer and how it governs the drag coefficient of a sphere was published by Achenbach [18]. The experimental data, collected using hydraulically-smooth metal spheres, are reproduced in Figs. 5 and 6 and shown as open circles (and marked *smooth* in the legend). Note that the shading, roughness data, and other features in these figures are discussed further below. The drag coefficient (C_d) as a function of the Reynolds number (Re) is shown in Fig. 5; the angle of boundary-layer separation, obtained from skin-friction measurements, is shown in Fig. 6. Cricket is typically played at $Re \sim 2 \times 10^5$, equivalent to 90 mph (145 km/h). For $Re < 2 \times 10^5$ (*subcritical* flow), Achenbach showed that the boundary layer is laminar and separates at $\theta_L \approx 80^\circ$. As Re is increased, the fluid-dynamic boundary layer enters a *critical* condition where C_d reduces markedly at $Re \approx 4 \times 10^5$; here the boundary layer is turbulent and the separation (detachment) points are displaced further downstream to $\theta_T \approx 120^\circ$. At higher Re the flow encounters the *supercritical* and ultimately a *trans-critical* regime. Here the attached boundary layer is predominantly turbulent and the angle of transition retreats upstream; the turbulence thickens the boundary layer, causing a gradual reduction in the angle of separation ($\theta_T < 120^\circ$).

The prominent fluid-dynamic feature at the critical Reynolds number is a *laminar separation bubble* (LSB) [19], where the laminar boundary layer separates, undergoes a transition to turbulence and re-attaches in turbulent form. The flow over a sphere in the critical region is illustrated as an inset in Fig. 6: θ_L , θ_R and θ_T indicate the laminar separation, turbulent reattachment, and turbulent separation points respectively for the bubble. Taneda [19] measured $92^\circ < \theta_L < 110^\circ$, $107^\circ < \theta_R < 127^\circ$ and $123^\circ < \theta_T < 147^\circ$ (depending on Re) for smooth spheres. An important point is that θ_T in the presence of a LSB is greater than that for the case with trans-critical flow. These angles are marked in Fig. 3 and it is noted that reverse swing is fundamentally caused by asymmetric turbulent separation angles on the seam and non-seam sides, the latter featuring the LSB.

2.4 Effect of surface roughness and cricket context

The critical speed for a smooth sphere in air at standard atmospheric conditions would be ~ 75 m/s (170 mph), well beyond the range capable of the fastest bowler. In practice, however, the air speed for transition to turbulence will be less than that measured on the smooth, machined, perfectly symmetric metal sphere used by Achenbach. Barton [20] measured this transition for a pristine cricket ball between $1.5 \times 10^5 < Re < 1.8 \times 10^5$, *i.e.* speeds $\sim 30 - 35$ m/s (60 – 78 mph). The reduced critical Re is expected due to inaccuracies in the general spherical shape of a manufactured cricket ball and surface irregularities and roughness.

Achenbach [21] extended his fundamental experiments to investigate the effect of surface roughness, which are also illustrated in Figs. 5 and 6 (adapted from Achenbach). A greater degree of roughness relative to the diameter was shown to significantly reduce the critical Reynolds number. The data was collected for $k/d = 250 \times 10^{-5}$ and 1250×10^{-5} and shown by triangular and square symbols, respectively, as marked in the legend. The elements of roughness disturb the boundary layer creating a transition to turbulence

at lower Reynolds number. The separation angle is a maximum at the critical Reynolds number and then decreases significantly in the trans-critical regime.

As discussed above, the relative size of the encircling seam was $k_s / d \sim 1000 \times 10^{-5}$. The size of the surface roughness (k_r) on the worn, scuffed balls was hugely variable, but estimated to an order of magnitude lower. These relative dimensions are broadly represented by the two sizes of roughness tested by Achenbach and shown in Figs. 5 and 6. Note Achenbach [21] tested a more comprehensive range ($k / d = 25 \times 10^{-5}$, 150×10^{-5} , 250×10^{-5} , 500×10^{-5} and 1250×10^{-5}), but only two are reproduced here for clarity.

Consider the fluid dynamics in the context of the start of a cricket match with a fast bowler operating at 90 mph, $Re \sim 2 \times 10^5$. With a new ball, the bowler is seeking CS (Fig. 1). Figure 6 shows the separation angle on the seam side at $\theta_T = 100^\circ$ and the non-seam side $\theta_L = 82^\circ$ and the range for CS for a smooth ball is high-lighted in red.

Consider now the situation later in the match with a worn ball where the relative roughness on the non-seam side has increased to $k / d = 250 \times 10^{-5}$. At the same bowling speed, Reynolds number and seam orientation there is now turbulent flow on both hemispheres; however, $\theta_T = 118^\circ$ on the non-seam side and the pressure asymmetry and consequently swing, is reversed. The range for RS for a worn/aged ball is highlighted in blue. Note that Achenbach's data suggests that a hydraulically-smooth cricket ball (*i.e.* $k / d \rightarrow 0$ on the non-seam side) should experience RS at $Re > 3.5 \times 10^5$ (160 mph). The new data collected and presented here shows a new cricket ball experiencing RS at $Re > 2.5 \times 10^5$, as the leather has a small degree of inherent roughness. In addition to the surface irregularities, manufactured cricket balls also feature two secondary seams (internally stitched and situated at 90° to the primary seam) and embossed logo that can influence the surface texture. Here is a brief summary of Fig. 6. The red region is where the turbulent-separation-angle on the seam side is greater than the *laminar*-separation-angle on the non-seam side. The blue region is where the turbulent-separation-angle on the non-seam side is greater than the *turbulent*-separation-angle on the seam side. The red region thus corresponds to CS and the blue region corresponds to RS. The shape, surface and seam of a cricket ball is modified as the game progresses and the ball ages. The seam may become less prominent during the course of play, but it is still obtrusive in terms of tripping the boundary-layer to turbulence, and so the flow is always turbulent on that hemisphere. The condition of the non-seam side of the ball is critical. This side of the ball receives the attention of the fielders and RS is a consequence of the right circumstances of surface roughness and Reynolds number to form the laminar separation bubble. In Fig. 6, the difference between RS and CS may be visualised by the difference between the blue and red boundaries and the data for $k / d = 1250 \times 10^{-5}$.

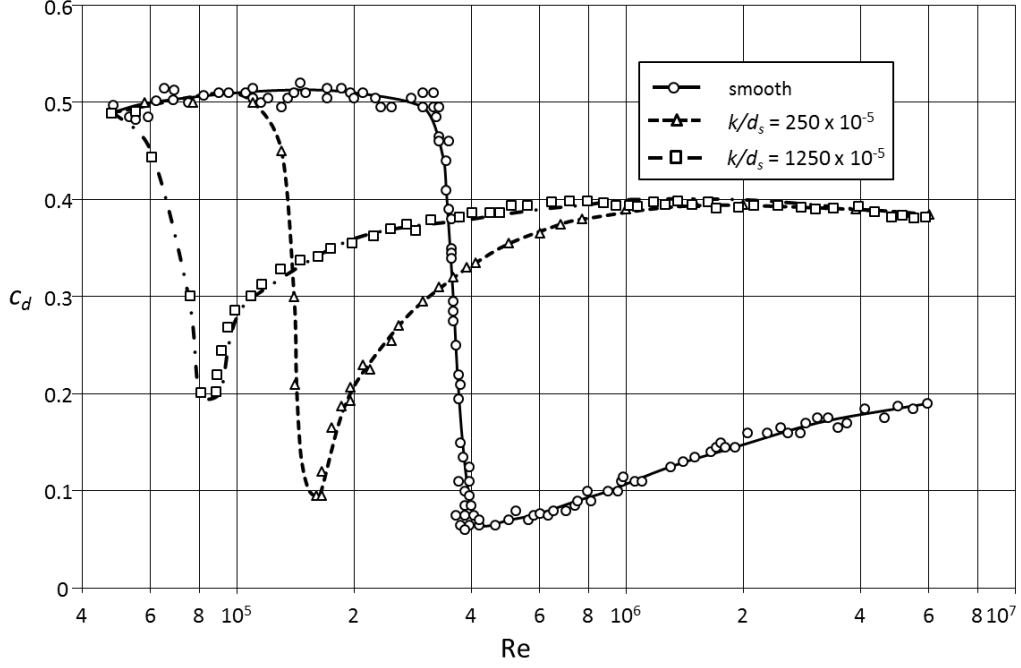


Figure 5: Variation of the drag coefficient with the Reynolds number for smooth and roughened spheres.

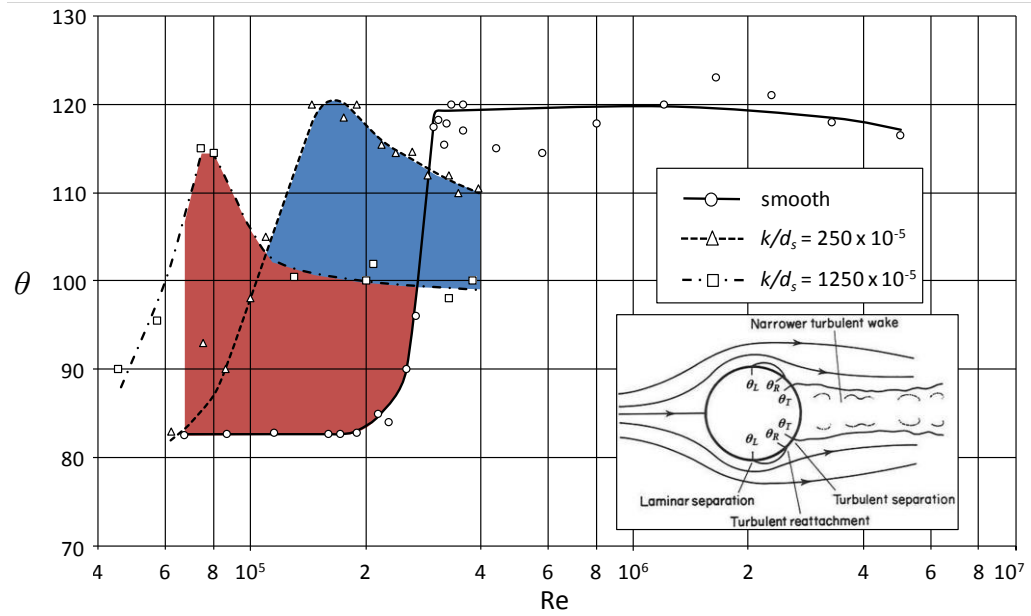


Figure 6: Variation of separation angles (with respect to the stagnation point) for smooth and roughened spheres. Red represents the difference in separation angle on either side of the ball resulting in CS, while blue will result in RS. For a given Reynolds number (bowling speed), the ball will be subjected to CS or RS depending on surface roughness. Squares – representative of seam roughness, Circles – representative of smooth non-seam side, Triangles – representative of worn non-seam side roughness.

3 Methods

Experiments were conducted in the University of Bath open-loop wind tunnel, with a maximum speed of 45 m/s (100 mph). The tunnel featured a square test section measuring 304×304 mm and a working length of 0.9 m; the blockage with the cricket ball installed was less than 5%.

The experimental configuration is illustrated in Fig. 7. A strain gauge was used to measure the side force Z perpendicular to the flow. The gauge was located on a supporting cantilever beam, which acted as an aerodynamic sting. It is common practice to use the side force in non-dimensional terms [e.g. 10, 13] by dividing by the projected area of the ball and the dynamic head of the fluid as shown in Eq. (1):

$$C_Z = \frac{8Z}{\rho U_\infty^2 \pi d^2} \quad (1)$$

The aerodynamic sting was positioned within the wake with the vertical beam 255 mm behind the ball in order to ensure minimal influence on the flow. The dimensions of the cantilever were designed to avoid resonance and vibration from the wind tunnel, and to maintain sensitivity to low side forces. A binocular design was used to exaggerate strain locally. A 3-D printed aerofoil fairing was mounted over the vertical support to minimise any upstream influence on the airflow around the ball.

In all experiments, the seam was set at an angle of incidence of 15° to the flow.

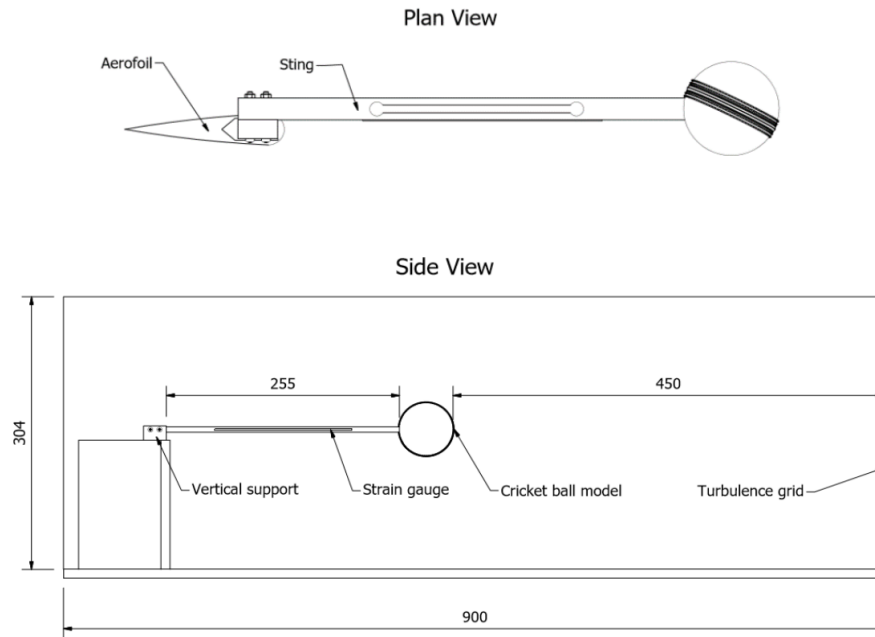


Figure 7: Experimental test configuration (flow from right to left). All dimensions in mm.

A signal generator was used to control the speed of the wind tunnel to help achieve accurate, repeatable test conditions. This was programmed to create a stepping ramp function that increased the speed of the wind tunnel from zero to its maximum, holding the velocity for 10 seconds at each increment. Data was acquired at 1000 samples every 0.3 seconds, with the results averaged over 10 seconds to take vibrational effects into account. The effects of hysteresis were tested to ensure that there was no difference in the results if measured from a velocity of 0 – 100 mph or decreased from 100 – 0 mph; no discernible difference was found.

3.1 Humidity levels

The humidity in the wind tunnel was controlled by initially introducing moisture into the air, then subsequently reducing the moisture content using a dehumidifier. The humidity levels were measured using a Testo 608-H1 thermohygrometer. The experiments were conducted at three humidity levels of 34, 51 and 73%.

3.2 Turbulence Grid Design

The design and manufacture of the turbulence generation grid used in the experiments reported here was based upon research and analytical correlations produced by Roach [22]. An ‘SMS’ grid (square-mesh array of square bars) was used to produce ‘nearly isotropic’ turbulence in the wind tunnel.

In order to match the turbulence intensity using a grid, an analytical correlation found by Roach [22] was used. It was determined that the critical design parameter was the length-scale of the wind tunnel, which was defined as the ratio of the distance of the test object downstream of the grid (x_T) to the critical diameter of the grid (d_g). The critical length was fixed at 450 mm from the start of the working section to the front of the ball (Fig. 7). Using Eq. (2), a theoretical value of 3.15% turbulence intensity (Tu) was found for a grid length of $d_g = 3$ mm. It was decided that this increase in turbulence would be satisfactory to replicate the required atmospheric turbulence within the wind tunnel.

$$Tu = \frac{u'}{U_\infty} = 1.13 \left(\frac{x_T}{d_g} \right)^{-5/7} \quad (2)$$

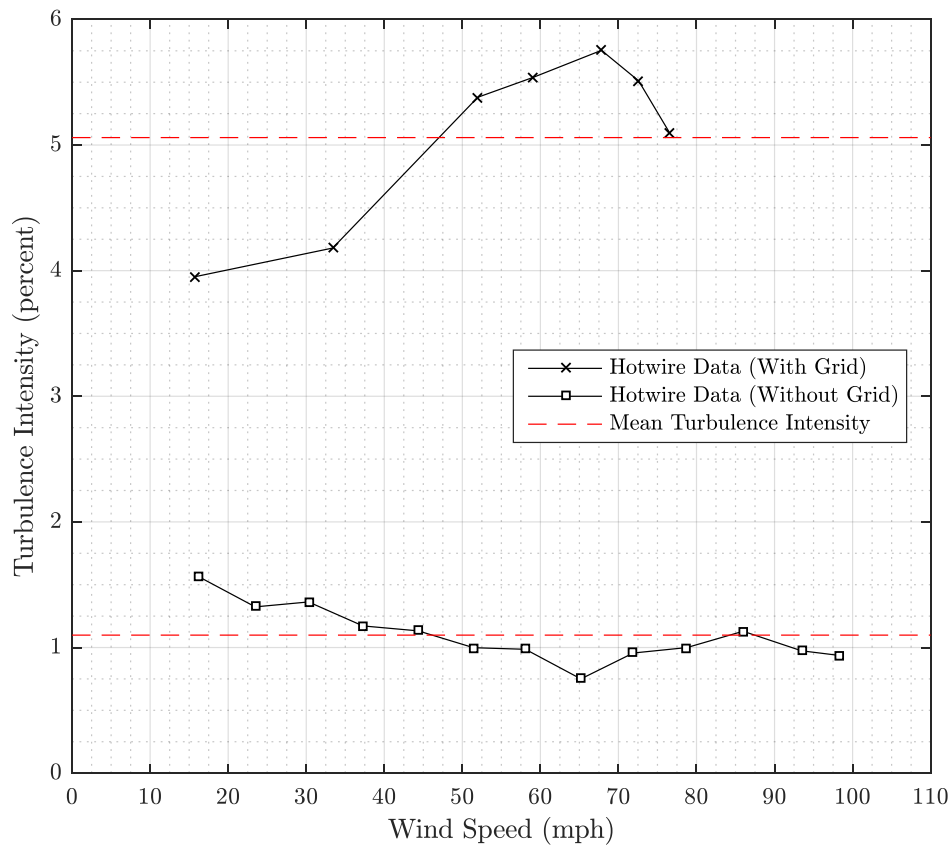


Figure 8: Turbulence intensity before and after installing the grid in the wind tunnel

Before fitting the grid into the wind-tunnel, an experiment was conducted to measure the background level of turbulence in the wind tunnel across the velocities in question. A hot-wire anemometer was inserted into the centre of the flow at the point where the cricket ball would usually be positioned. This was found to have a mean of $u'/U_\infty \approx 1\%$ as observed in Fig. 8.

An increase of more than 3% from the base-level wind tunnel turbulence intensity was expected from the grid, as predicted from Eq. (1). However, as shown in Fig. 8, the turbulence grid in fact increased the mean turbulence intensity in the tunnel to $u'/U_\infty \approx 5\%$. This additional turbulence can be explained as Roach's work produced lines of best fit to form 'over-arching' empirical correlations. As a result, some deviation from

the prediction might be expected. Using this grid, an increase in u'/U_∞ of 4% was measured, which produced the desired turbulence.

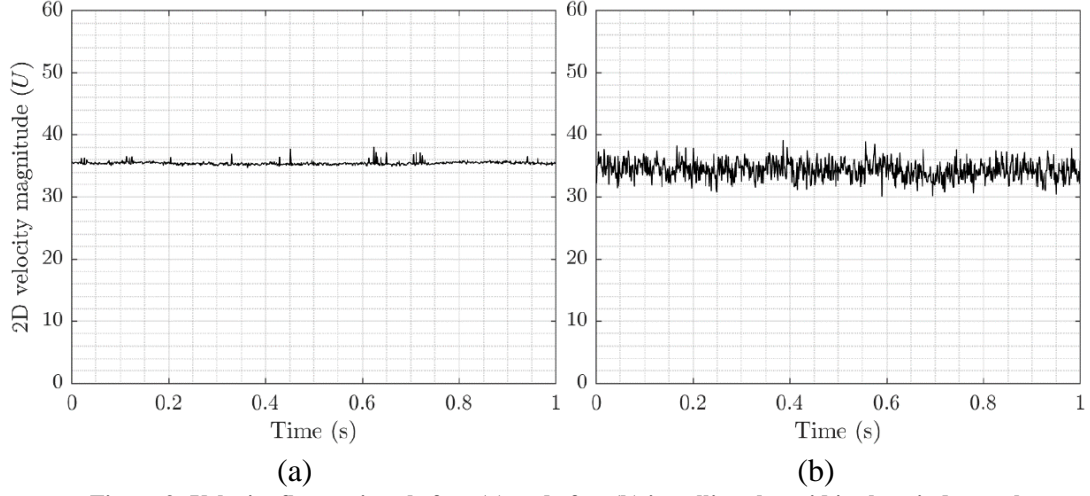


Figure 9: Velocity fluctuations before (a) and after (b) installing the grid in the wind tunnel

Figure 9 shows the difference in the fluctuating form of the turbulence before and after inserting the grid. These velocity fluctuations correspond to mean velocities of approximately 36 m/s (80.5 mph).

The length-scale of the turbulence produced was also a major factor in representing atmospheric conditions accurately. Roach's correlation for integral length-scale (Λ_x) growth downstream of the grid is shown in Eq. (3):

$$\frac{\Lambda_x}{d_g} = 0.2 \left(\frac{x_T}{d_g} \right)^{1/2} \quad (3)$$

Using this correlation, the integral length scale of the turbulence was calculated to be 7.35 mm, approximately 10% of the ball diameter. This shows that the turbulence around the ball is isotropic, which in theory should produce the desired disruptive effect on the boundary layer.

3.3 Ball Tampering and Polishing

Match-play ball tampering and polishing was simulated for some of the experiments with the assistance of a first-class cricketer. Here the ball was vigorously polished on the smooth (non-seam) side with sweetened saliva, simulating a fielder in a match context. It is difficult to quantify the change in surface finish of the ball, but there was a dramatic visual difference in shine.

4 Experimental results and discussion

In this section measurements of side-force (*i.e.* swing) for cricket balls are presented over a range of bowling speeds encountered in a professional match, assessing a variety of features. In Section 4.1 red *Dukes* balls aged under first-class match conditions are used to assess the effect of surface wear (*i.e.* number of overs bowled). In Section 4.2,

aged pink *Kookaburra* balls supplied by the MCC from an experimental day-night match in Abu Dhabi were tested. In Section 4.3, the aerodynamic performance of pristine, out-of-the-plastic-wrapper, red and pink *Dukes* balls and a white *Kookaburra* ball are compared. In Section 4.4 the effect of illegally polishing the ball with sweet saliva is investigated and the effect of ball tampering with sand paper is considered. In Sections 4.5 and 4.6, the effect of atmospheric humidity and turbulence are explored respectively.

4.1 Aged red *Dukes* balls, worn during first-class play

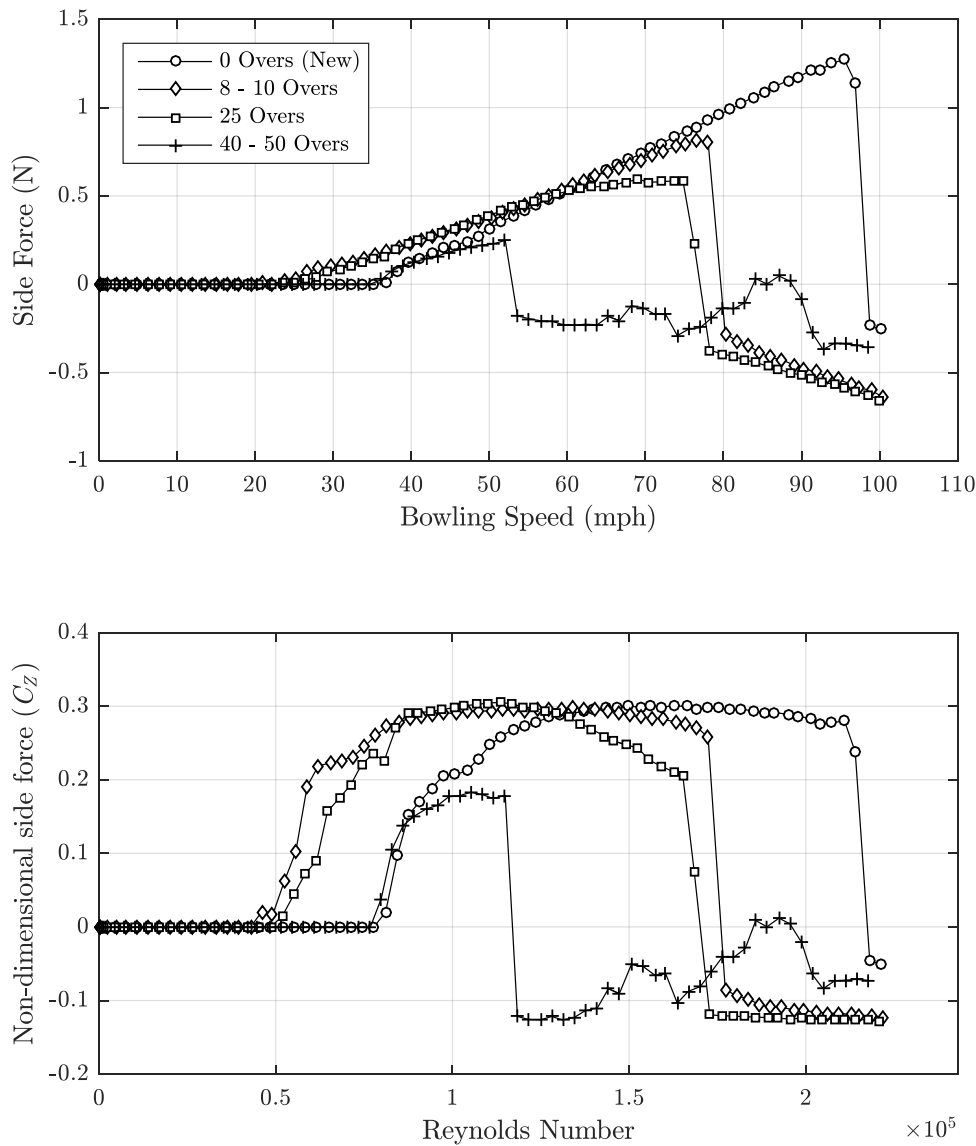


Figure 10: (a) Variation of side force with speed and (b) non-dimensional side force (C_z) with Reynolds number (Re) for red *Dukes* balls at different stages of wear

Figure 10 shows the variation of side force with air-speed and the non-dimensional side force (C_z) with Reynolds number. C_z is defined above in Eq. (1). The data was collected

using four red *Dukes* balls: a new one and three aged 8-10, 25 and 40-50 overs under first class conditions. The bowling speed is shown in miles per hour (mph) to present the data in terms with which the cricket audience would be familiar. For consistency, all experiments were conducted with the seam angle set at 15° to the air stream. Positive values of C_z correspond to conventional swing, while negative values correspond to reverse swing.

Note that a new, pristine, ball encounters RS at 95+ mph. As the ball ages, the onset of the RS regime begins at a lower speed.

The non-dimensional side-force data in the study by Shah *et al.* [23] can be compared with the “new ball” data the authors presented above. Over the range for conventional swing $1.3 \times 10^5 < \text{Re} < 1.7 \times 10^5$ [23] measured a relatively constant $C_z = 0.3$, which agrees well with the data presented in Fig. 10 (b). The comparison is good despite differences in the seam angle to the flow (30° for [23]) *versus* 15° used here; also, the ball used in the study by Shah *et al.* [23] was manufactured by *SG*, not *Dukes*.

For all balls in the regime $\text{Re} < 0.4 \times 10^5$, the side-force is zero as the flow is laminar on both hemispheres with symmetric boundary-layer separation. The increase in C_z with increasing Re indicates CS with transition to turbulent flow on the seam side. The transition point varies with age and is probably influenced by both the surface condition and how the seam has worn. At higher Re , there is a dramatic reduction in C_z and a reverse in the direction of force as the ball encounters RS. The variation of C_z with Re is qualitatively similar for all specimens; with the exception of the most-worn case (40-50 overs), the balls all feature a maximum $C_z = 0.3$. The critical Re marking the regime for RS reduces with increased roughness that precipitates the LSB on the non-seam side and reverses the asymmetry of the angles for turbulent separation on the two hemispheres. The magnitude of C_z for RS is significantly less than that for CS (typically -0.1 vs. 0.3). The magnitude of C_z for RS is larger for balls with more wear as the LSB gradually translates upstream with increasing roughness, creating greater pressure asymmetry.

In the context of a match, consider a bowler operating with an out-of-hand delivery between 80-90 mph, with the ball decelerating with drag during flight. The bowler will generate CS with the *new ball*, experiencing maximum side force (and hence maximum sideways deviation in trajectory) at higher bowling speeds. Reverse swing would occur if speeds greater than 100 mph were possible. Consider now the ball *aged 8-10 overs*. In the speed range 80-90 mph, CS has been lost; instead RS occurs but the sideways deviation would be less than that with the new ball as C_z is smaller in magnitude. Only the faster bowlers (those near 90 mph) will generate RS because if the ball decelerates below 80 mph, the net sideways deviation is suppressed through a combination of both CS and RS. The ball *aged 25 overs* will experience RS, with CS only effective for speeds less than 78 mph. The ball *aged 40-50 overs* will experience RS in the range 80-90 mph, but with lower C_z the consequences will not be as effective as the ball aged 25 overs; CS is lost at speeds greater than 52 mph.

It should be noted that during the course of play, a swing bowler, as discussed earlier, usually imparts a small degree of backspin on the ball. The influence of this rotation on the formation and stability of the separation bubble was not tested in the experiments reported here.

4.2 Aged pink Kookaburra balls

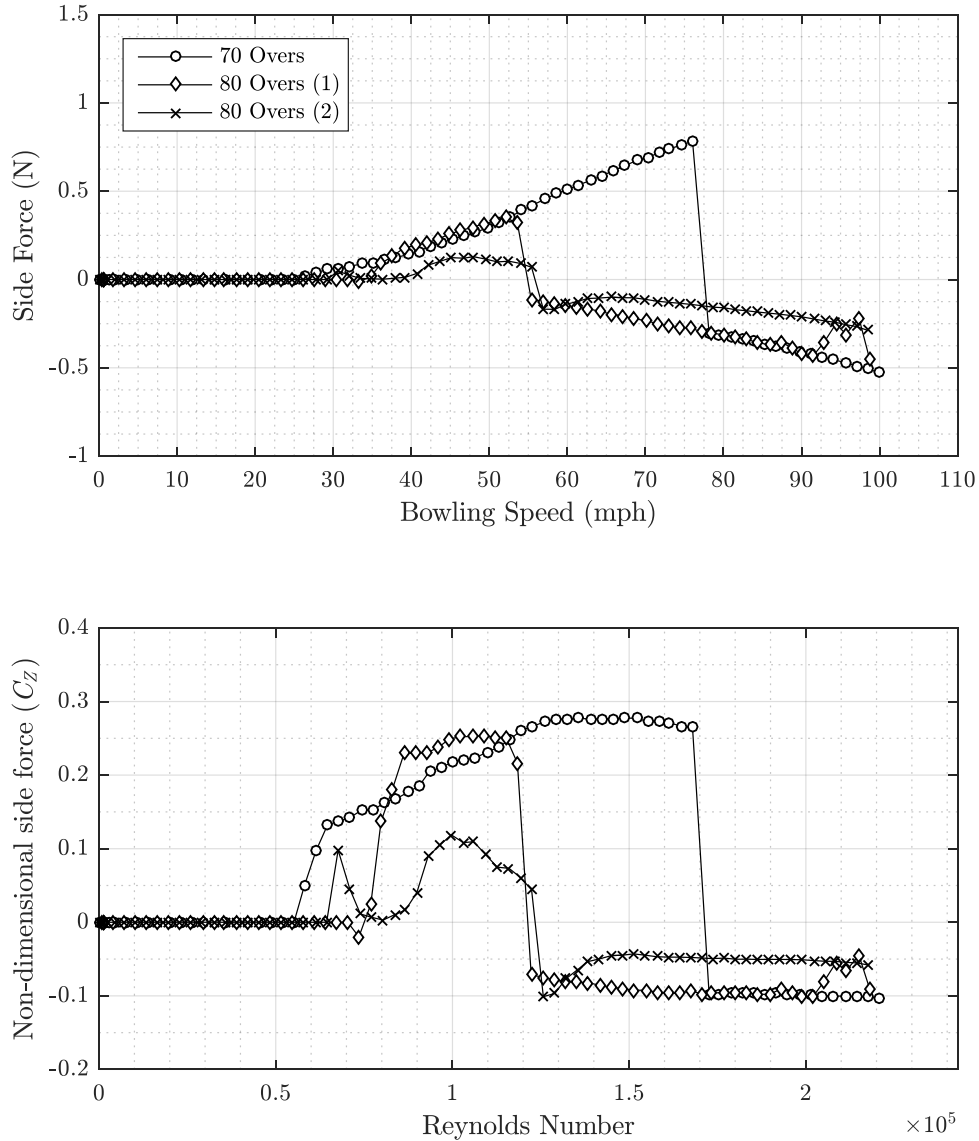


Figure 11: A comparison of older pink balls Kookaburra at different states of wear

Figure 11 shows a comparison between the three pink *Kookaburra* balls, one aged 70 overs and two aged 80 overs. One of the 80-over balls, marked (2) in the legend, was severely scuffed and less well-maintained than the other as clearly shown in Fig. 4 and Appendix 2. As discussed above, these balls were used in an experimental MCC day-night match in Abu Dhabi. The aerodynamic performance is qualitatively similar to the red *Dukes* balls presented in Fig. 10. The 70-over ball has a peak magnitude in conventional swing equivalent to $C_z = 0.28$, and swings in the reverse direction at speeds above 78 mph with a constant $C_z = -0.1$ virtually independent of increasing Re. The better-maintained ball aged 80 overs encounters reverse swing at 55 mph. The ball

with the most severe deterioration does not exhibit effective CS and the degree of RS is less than that for the better-maintained balls. In a cricket match, the fielding captain seeking to exploit lateral movement would be advised to take the new ball (due at 80 overs) with CS for bowlers operating between 80-90 mph.

4.3 Comparison of new red, pink and white balls

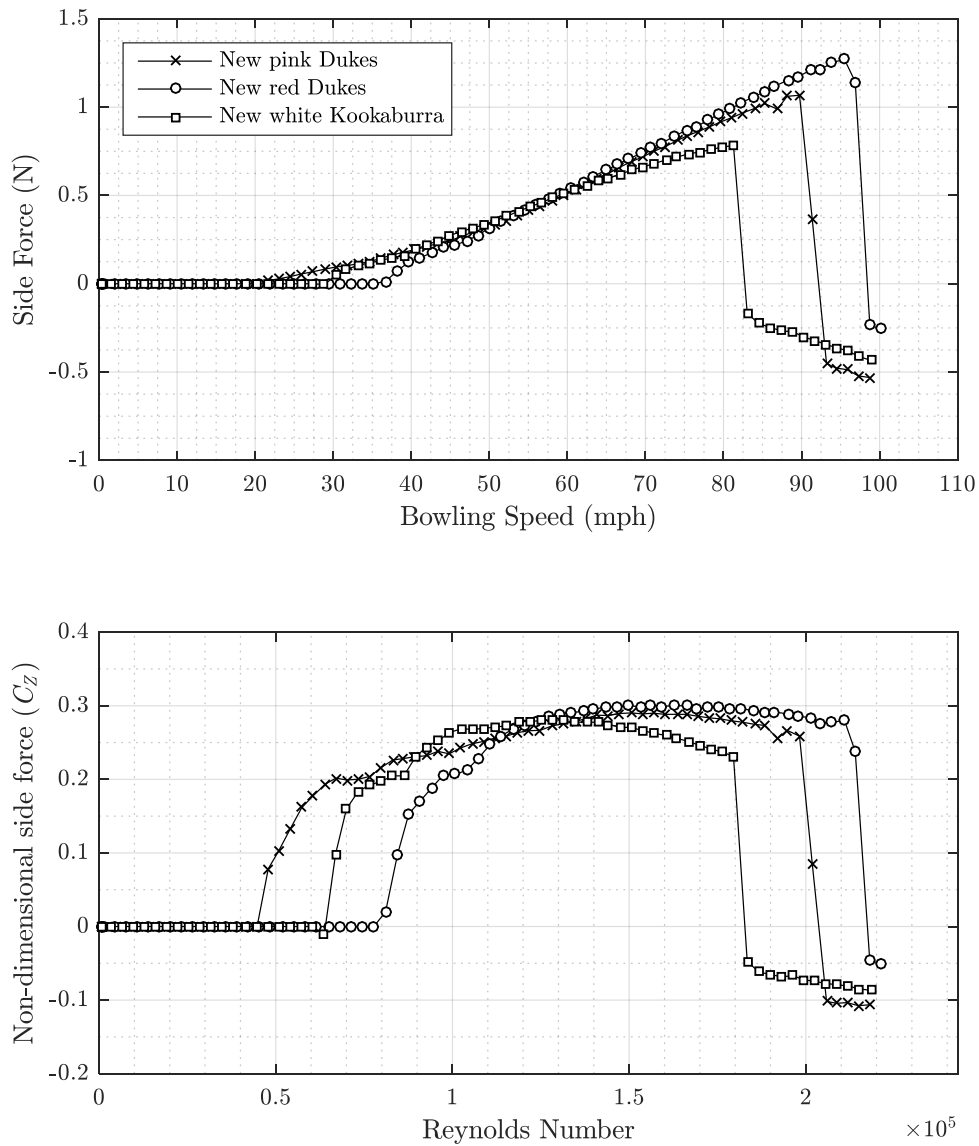


Figure 12: A comparison of different types of new balls

The aerodynamic performance of red and pink *Dukes* balls and a white *Kookaburra* ball were compared, all at a common seam angle of 15° . These were purchased from the manufacturers in pristine condition and represent the balls available at the start of the match or after 80 overs of play. The balls have different-sized seams with subtle variations in the texture of the leather.

The experimental data is illustrated in Fig. 12. The increase of C_z from zero marks the onset of the regime for CS with turbulent flow on the hemisphere with the seam. There are surprising differences in this lower critical Re, but from the practical perspective of a cricket match, all three balls swing conventionally beyond 40 mph. In the bowling range 80-90 mph, the two *Dukes* balls exhibit CS with the abrupt transition to RS beyond 90 mph. The critical speed for this transition is lower for the pink ball and probably caused by slight differences in the surface texture that influence the fragile LSB on the non-seam side. There may be differences in the manufacturing technique and the lacquer used for the two balls, but no conclusive evidence has been found indicating differences other than the colour. Experiments with a larger number of samples is required to further the investigation.

The aerodynamic performance of the white *Kookaburra* ball is very different. The transition from CS to RS occurs at 82 mph. Further, the magnitude of C_z is generally less than that of the *Dukes* balls in both the CS and RS regimes. It is worth noting that the *Kookaburra* ball has a prominent secondary seam (a 0.5 mm gap dividing each hemisphere into halves) as shown in Appendix 2. The fluid-dynamic boundary layer will be affected by these secondary seams with an influence on the critical Re.

Consider the trajectory of a cricket ball that will slow with drag in its flight from the bowler's release towards the batsman. A top-class fast bowler typically releases the ball between 80-90 mph. A simple one-dimensional numerical solution of the trajectory based on a drag coefficient of 0.5 (measurements of drag were made as part of this study but not presented here, however this is consistent with [13]) shows that the ball will slow by approximately 15% from the point of release to reaching the stumps. At a bowling speed of 85 mph out of the hand, the ball will therefore slow to 72 mph by the time it reaches the batsman. The *Dukes* ball will experience CS at near maximum C_z and with a consistent direction of deviation during flight. The bowler using the white *Kookaburra* ball will experience a combination of CS and RS (both at lower C_z in comparison to the *Dukes* ball) with less net lateral movement.

The above discussion leads to the phenomenon of *late swing*. To quote a sentence highlighted in bold from the 1952 MCC Cricket Coaching Book [24]: 'Nearly all great batsmen are agreed that it is the ball that "runs away from them" late in its flight that is the most dangerous.' Consider again Fig. 10, in particular the data for the ball aged 8-10 overs. A ball that decelerates below 80 mph late in its trajectory will suddenly experience this late swing.

4.4 Illegally polishing the ball with sweet saliva

The shine on a *Kookaburra* ball, used by both South Africa and Australia does not persist as long as that on the *Dukes* ball. In the 2016 Australia *versus* South-Africa Test series, captain Faf Du Plessis received an official ban from the ICC for applying saliva to the ball with a mint in his mouth. Generally such practice is an attempt to coat the non-seam side of the ball with a shiny, smooth, persistent lacquer that will inhibit the transition from laminar to turbulent flow. *Vaseline* and sun-cream have also been suspected foreign ingredients in such attempts.

The effects of polishing the non-seam side of an aged ball with sweet saliva was investigated with the assistance of a former first-class bowler, as discussed in Section 3.3. A red *Dukes* ball aged approximately 25 overs was used as the specimen.

The results are illustrated in Fig. 13. In its un-polished state, the ball swings in a conventional manner, but only for bowling speeds less 75 mph. In a professional match, bowlers will seek effective swing at higher speeds. In the polished state, a greater degree of CS is experienced and the more effective swing persists to higher speeds. In the polished state, the ball is well suited for *late swing*.

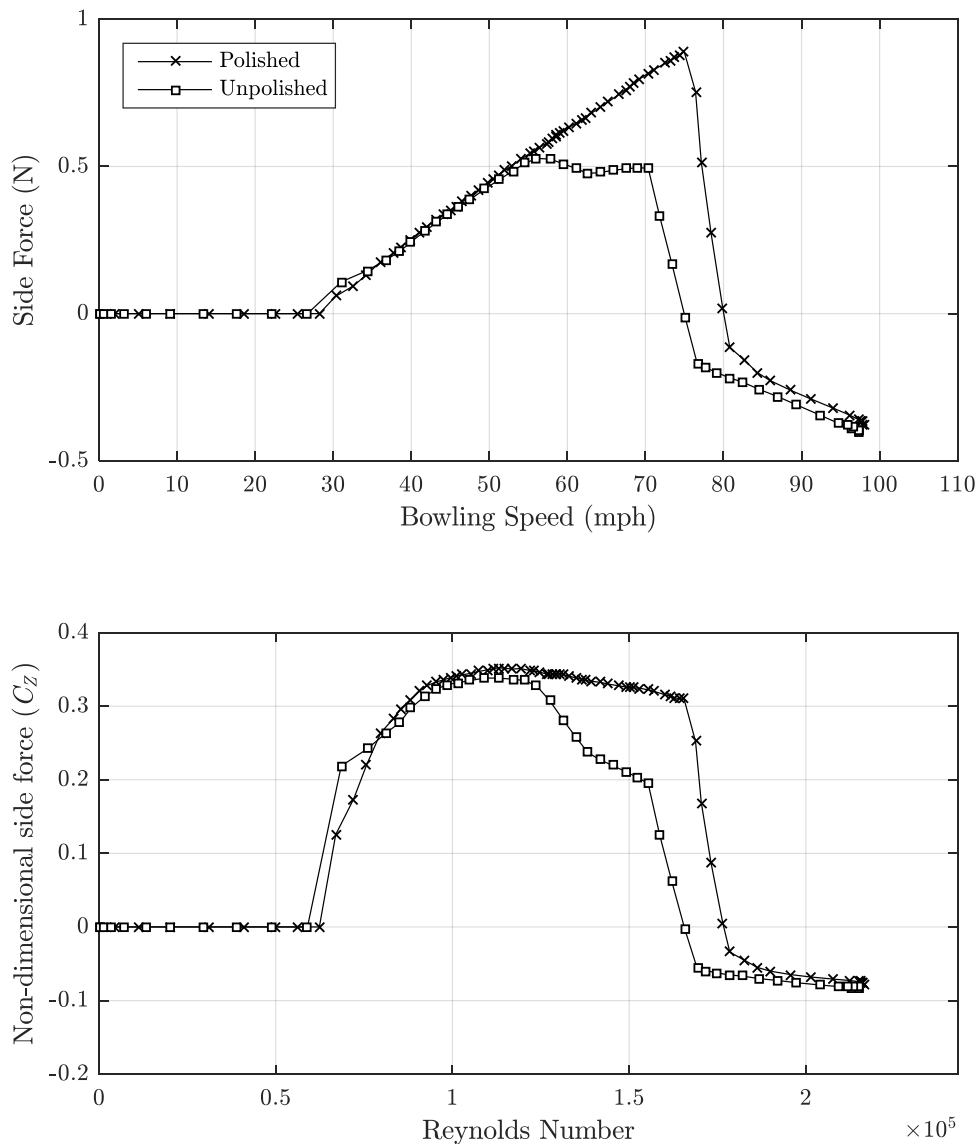


Figure 13: The effect of using sweet saliva to polish the ball

The 2018 South-Africa *versus* Australia series created a media storm with three Australian cricketers receiving lengthy bans for ball tampering using sand-paper. The

Kookaburra ball was being illegally roughened to accelerate and enhance the effect of reverse swing.

Using sand-paper to strategically roughen the non-seam side of the ball is consistent with the evidence discussed above. The effect will enhance the onset and degree of RS with an aged ball. More vitally, the bowling speed for effective RS would be brought within the effective bowling range between 80-90 mph. Thus, ball tampering is a ploy to summon RS from an aged ball that has lost its ability for effective CS for the fast bowler operating between 80-90 mph. The shine on a *Kookaburra* ball, used by both South Africa and Australia, does not persist and this may be a factor in the bowlers seeking RS.

4.5 Atmospheric conditions - humidity

As discussed in Section 3, experiments were conducted at humidity levels of 34, 51 and 73%. The swing of a new, red *Dukes* ball under these conditions is shown in Fig. 14. There is no significant effect of humidity in terms of the magnitude of swing, nor the critical Re for transition from CS to RS.

Atmospheric conditions are a common topic of discussion in cricketing circles with wisdom and experience suggesting that swing is promoted in humid conditions. The above experiments have isolated humidity from other environmental features that might contribute to this experience. Humid circumstances are often associated with cloud cover (discussed in the next section) and moisture may affect wear and polishing during play.

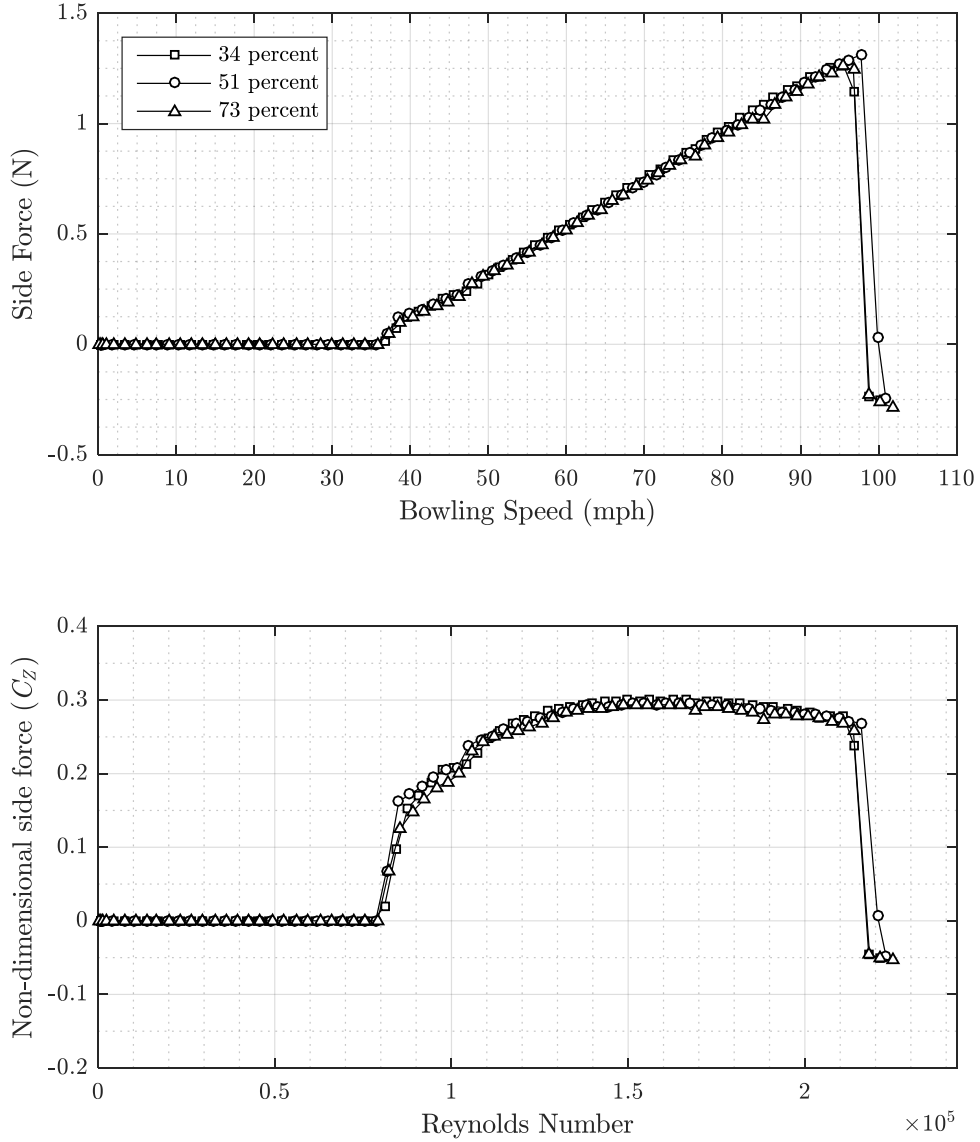


Figure 14: The isolated effect of humidity on swing for a new, red Dukes ball

4.6 Atmospheric conditions – micro-turbulence

Experience suggests that swing tends to happen on cloudy days but not sunny days [12]. Clearly, the formation of the laminar boundary layer on the smooth side of the ball is crucial for effective CS; the fragile laminar boundary layer must form naturally and this is not possible in the presence of turbulence. Meteorological studies have shown that the direct irradiation of the sun creates horizontal and vertical velocity fluctuations near the ground. Ibbetson [11] used sensitive hot-wire anemometry to capture the fluctuating convective micro-turbulence at a height of 2 m above a meteorological site. The vertical velocity fluctuations were measured to be typically ± 0.75 m/s. As discussed in Section 3.1, a turbulence grid was designed to reproduce these velocity fluctuations that at an air-speed of 85 mph (38 m/s) equated to 4% turbulence intensity – Eq. (2). The actual

measured level of turbulence was 5% with an integral length scale of 7.3 mm (*i.e.* 10% of the ball diameter) – Eq. (3).

Experimental measurements of side-force were conducted with and without the turbulence grid. The swing of a new, red *Dukes* ball under these conditions is shown in Fig. 15. The turbulence created by the grid has virtually eliminated the side-force, indicating that there is turbulent flow on both hemispheres. At larger Re , there is a small degree of RS possibly associated with the upstream movement of the separation angle from its maximum value of $\theta_T = 115^\circ$ at $Re = 0.8 \times 10^5$ (see Fig. 6) on the seam side of the ball. Consider the data in the setting of a cricket match with a new-ball bowler

operating at 80-90 mph: if the micro-turbulence were caused by the heating of a hot sun on the wicket, there would be no swing; on a cloudy day the ball will swing.

In a day-night match, the quiescent environment associated with twilight may suddenly conjure swing for the pink ball.

As a note of caution, the general characteristics, intensity and length scale of the turbulence created in the wind tunnel experiments simulate, but not necessarily replicate, those experienced in the varied possibilities of match scenarios.

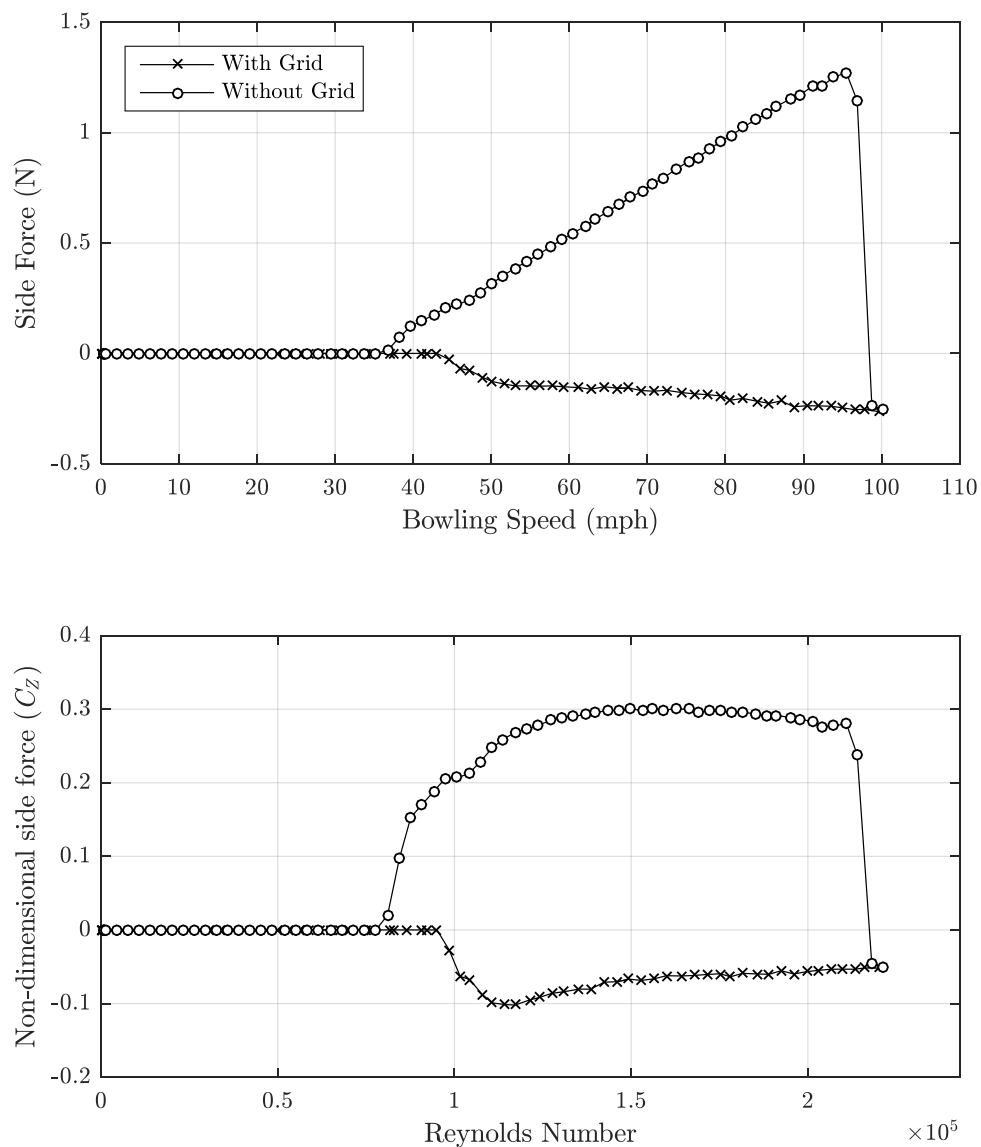


Figure 15: The effect of micro-turbulence on swing for a new, red Dukes ball

5 Conclusions

“Cricket is an Indian game accidentally discovered by the English,” states Ashis Nandy in his delightful book, *The Tao of Cricket* [25]. Cricket is also a game accidentally played at a Reynolds number of 2×10^5 . With stitching and seam, with wear and tear accumulated by means fair and foul, a cricket ball bowled with great skill can be made to swing. At 80-90 mph, the swing is governed by the boundary-layer on the non-seam side of the ball: this will be laminar if the surface is smooth and there is no micro-turbulence to disturb it, bringing conventional swing (CS); the boundary-layer will experience a critical condition if the surface is appropriately rough, bringing reverse swing (RS). The fundamental fluid dynamics can be explained by experiments conducted by a German physicist in the 1970s.

Using balls worn under match conditions and insight from a professional cricketer, factors affecting swing were investigated. Ten cricket balls of different colours from different manufacturers were tested aerodynamically in a wind tunnel where both CS and RS were measured. The data collected supports the theory that swing is caused by the asymmetric separation of the fluid-dynamic boundary layer, with RS featuring a laminar separation bubble on the non-seam side. At 80-90 mph, the roughness of the surface of the ball was found to govern the direction and degree of swing achieved. The results were consistent with expectations from a match situation: the new ball experienced CS but this swing was lost as the ball aged while older, worn balls effectively operated with RS. Illegal tampering of the non-seam side was shown to influence swing: sweet saliva was shown to promote laminar flow, hence prolonging CS as the ball aged.

The question of the effect of weather conditions on swing was investigated, but not resolved conclusively. Atmospheric humidity in isolation showed no direct link to increased swing. A turbulent mesh was used to simulate turbulent convection currents rising from a cricket pitch irradiated by the sun. The turbulence destroyed the laminar boundary layer on the non-seam side of the ball, suggesting cloudy days support swing.

Recommended future work would be to assess the presence of the laminar separation bubble on a rotating cricket ball, rather than one in a fixed position. The authors have plans to investigate this phenomenon using optical flow measurement techniques.

Nomenclature

C_d non-dimensional drag-force, $C_d = \frac{8D}{\rho U_\infty^2 \pi d^2}$

C_Z non-dimensional side-force, $C_Z = \frac{8Z}{\rho U_\infty^2 \pi d^2}$

d diameter

d_g critical diameter of turbulence grid

D drag force

k size of roughness element

k_r surface roughness

k_s	seam roughness
Re	Reynolds number $= \frac{\rho v_{\infty} d}{\mu}$
Z	side force
Tu	turbulence intensity
U_{∞}	free-stream velocity
u'	standard deviation of velocity fluctuations
x_T	distance of test object downstream of turbulence grid
θ	separation angle from the stagnation point
θ_L	laminar separation angle
θ_R	turbulent reattachment angle
θ_T	turbulent separation angle
Λ_x	integral length scale growth
μ	dynamic viscosity
ρ	density

References

- [1] Wynne-Thomas, P., The history of cricket: from the weald to the world, Norwich : Stationery Office, 1934.
- [2] Barkla, H. M. and Auchterlonie, L. J., "The Magnus or Robins effect on rotating spheres," Journal of Fluid Mechanics, vol. 47, no. 3, pp. 437-447, 1971.
- [3] Phillips, E., Davids, K., Renshaw I. and Portus, M., "The Development of Fast Bowling Experts in Australian Cricket," Talent Development & Excellence, vol. 2, p. 137–148, 2010.
- [4] Cox, G., Cricket Ball. The Heart of the Game. Bloomsbury Academic Press, 2019
- [5] Brearley, M., On Cricket, Constable, 2018
- [6] Cooke, J. C., "Boundary Layer and "Seam" Bowling," The Mathematical Gazette, vol. 39, no. 329, pp. 196-199, 1955.
- [7] Lyttleton, R. A., "The swing of a cricket ball," Discovery, vol. 18, pp. 186-191, 1957.
- [8] Bradman, D. G., "The Art of Cricket," Hodder & Stoughton, London, 1958.
- [9] Mehta, R. D. An overview of cricket ball swing. Sports Engineering 2005; 8: 181–192.

- [10] Scobie, J. A., Pickering, S. G., Almond D. P. and Lock, G. D., "Fluid dynamics of cricket ball swing," *Journal of Sports Engineering and Technology*, vol. 227, pp. 196-208, 2013.
- [11] Ibbetson, A., "Some aspects of the description of atmospheric turbulence," *Weather*, vol. 33, no. 10, pp. 369-382, 1978.
- [12] Wilkins, B., *The Bowler's Art*, London: A & C Black, 1991.
- [13] Deshpande, R., Shakya, R. and Mittal, S., "The role of the seam in the swing of a cricket ball," *Journal of Fluid Mechanics*, vol. 851, p. 50–82, 2018.
- [14] Horlock, J., "The swing of a cricket ball," *Mechanics and Sport*, pp. 293-303, 1973.
- [15] Sherwin, K. and Sproston, L. J., "Aerodynamics of a cricket ball," *Int. J Mech.* vol. 10, no. 2, pp. 43-50, 1982.
- [16] Daish, C., "The Physics of Ball Games," *English Universities Press*, pp. 168-174, 1972.
- [17] Bentley, K., Varty, P., Proudlove, M. and Mehta, R., "An experimental study of cricket ball swing," *Imperial College Aero. Technical note 82-106*, 1982.
- [18] Achenbach, E., "Experiments on the flow past spheres at high Reynolds numbers," *J Fluid Mech.* 1972; 54(3): 565–575.
- [19] Taneda, S., "Visual observations of the flow past a sphere at Reynolds numbers between 10^4 and 10^6 ," *J Fluid Mech.* 1977; 85(1): 187–192.
- [20] Barton, N.G., "On the swing of a cricket ball in flight," *Proceedings of the Royal Society of London*, 1982, Series A 379, 109-131.
- [21] Achenbach, E., "The effects of surface roughness and tunnel blockage on the flow past spheres," *J Fluid Mech.* 1974; 65(1): 113–125.
- [22] Roach, P. E., "The generation of nearly isotropic turbulence by means of grids," *International Journal of Heat and Fluid Flow*, vol. 8, no. 2, pp. 82-92, 1987.
- [23] Shah, K., Shakya, R. and Mittal, S., "Aerodynamic forces on projectiles used in various sports," *Phys. Fluids* 31, 015106, 2019.
- [24] Anon. *The MCC cricket coaching book*, 1952 (Naldrett Press, London).
- [25] Nandy, A., *The Tao of Cricket*, Penguin, 1989.

Appendix 1

Figure	Description of Experiment	Balls Tested
Figure 10	Effect of aging under match conditions for red Dukes ball	New Red Dukes 8-10 Overs Red Dukes 25 Overs Red Dukes 40-50 Overs Red Dukes
Figure 11	Effect of aging (70+ overs) under match conditions for worn pink ball	70 Overs Pink Kookaburra 80 (1) Overs Pink Kookaburra 80 (2) Overs Pink Kookaburra
Figure 12	Effect of ball colour and manufacturer – new ball	New Red Dukes New Pink Dukes New White Kookaburra
Figure 13	Effect of polishing the ball	25 Overs Red Dukes
Figure 14	Effect of atmospheric humidity	New Red Dukes
Figure 15	Effect of freestream turbulence	New Red Dukes

Appendix 2



New Red Dukes



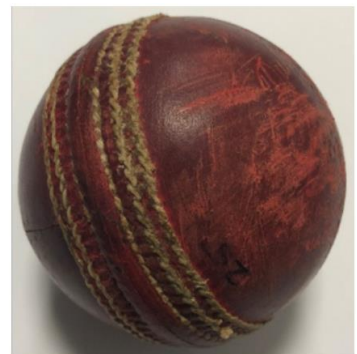
New Pink Dukes



New White Kookaburra



8-10 Overs Dukes



25 Overs Dukes



40-50 Overs Dukes



70 Overs Kookaburra



80 (1) Overs Kookaburra



80 (2) Overs Kookaburra

Ball Type	Colour	Condition	Description
Dukes Special County 'A' BSI-Grade 1	Red	New Red Dukes	No scuffs on either hemisphere, lacquer in excellent condition.
		8 – 10 Overs	Some light scuffs on the smooth side, heavy scuffs and a large gouge on the rough side.
		25 Overs	Well-polished smooth side, some mid-heavy scuffs on the rough side.
		40 – 50 Overs	General medium scuffs on both sides of the ball, no obvious features.
	Pink	New Pink Dukes	No scuffs on either hemisphere, lacquer in excellent condition.
Kookaburra Turf	Pink	70 Overs	No distinct differences between hemispheres, smooth with some discoloured leather.
		80 Overs (1)	Both sides very worn leather peeling off in places.
		80 Overs (2)	Poor condition, much leather peeling off each side and lots of bare patches.
	White	New White Kookaburra	No scuffs and lacquer intact, noticeably large secondary seam.